Effects of Brefeldin A on Endocytosis, Transcytosis and Transport to the Golgi Complex in Polarized MDCK Cells

Kristian Prydz,* Steen H. Hansen,‡ Kirsten Sandvig,* and Bo van Deurs‡

*Institute for Cancer Research at The Norwegian Radium Hospital, Montebello, 0310 Oslo 3, Norway; and ‡Structural Cell Biology Unit, Department of Anatomy, The Panum Institute, University of Copenhagen, DK-2200 Copenhagen N, Denmark

Abstract. We have studied the effects of brefeldin A (BFA) on endocytosis and intracellular traffic in polarized MDCK cells by using the galactose-binding protein toxin ricin as a membrane marker and HRP as a marker of fluid phase transport. We found that BFA treatment rapidly increased apical endocytosis of both ricin and HRP, whereas basolateral endocytosis was unaffected, as was endocytosis of HRP in the poorly polarized carcinoma cell lines HEp-2 and T47D. Tubular endosomes were induced by BFA both apically and basolaterally in some MDCK cells, comparable with those seen in HEp-2 and T47D cells. In addition, in MDCK cells, BFA induced formation of small (<300 nm) vesicles, labeled both after apical and basolateral uptake of HRP, as well as some very large (>700 nm) vacuoles, which were only labeled when HRP was present in the apical medium. In contrast, neither in MDCK nor in HEp-2 or T47D cells, did BFA have any effect on lysosomal morphology. Moreover, transcytosis in the basolateral–apical direction was stimulated both for HRP and ricin. Other vesicular transport routes were less affected or unaffected by BFA treatment. Two closely related structural analogues of BFA (B16 and B21), unable to produce the changes in Golgi and endosomal morphology seen after BFA treatment in a number of different cell lines, were also unable to mimic the effects of BFA on MDCK cells.

A well documented effect of the fungal metabolite brefeldin A (BFA)[1] on mammalian cells is rapid dissociation of proteins associated with the cytosolic face of the Golgi apparatus (7–9), and a subsequent retrograde movement of components of the *cis*-, medial, and *trans*-Golgi stacks back into the ER (6, 10, 17, 18, 24). However, markers of the *trans*-Golgi network (TGN), do not move along to the ER upon BFA treatment (5, 6, 18, 32).

Recently, it was reported that BFA transforms the morphology of endosomes, lysosomes, and the TGN in normal rat kidney (NRK) cells into more tubular structures (19, 44). Studies on the distribution of the TGN 38-protein have shown that BFA treatment may also give a more compact TGN 38 immunofluorescence around the microtubule organizing center (19, 28).

Two kidney epithelial cell lines (PtK and MDCK) have Golgi stacks that appear to be morphologically resistant to BFA (15, 16, 32). However, BFA treatment does cause formation of tubular endosomes in both cell lines, suggesting that the effect of BFA on endosomes is not directly coupled to the effect on the Golgi apparatus (15, 19).

In MDCK cells there are two distinct populations of early endosomes localized close to the apical and the basolateral surface domains, respectively. Markers of apical and basolateral endocytosis are therefore initially separated, before they enter mannose-6-phosphate receptor-rich late endosomes and lysosomes shared by the two pathways (3, 26, 42). Early apical and early basolateral endosomes display differences in their fusion machineries and in the way they handle internalized markers (2, 3, 26). We therefore found it of interest to examine if BFA had similar or different effects on endocytosis and intracellular traffic from the apical and basolateral surface domains of polarized MDCK cells.

We report here that BFA increases the endocytosis selectively from the apical surface of polarized MDCK cells. Moreover, transcytosis in the basolateral to apical direction is also increased by BFA.

1. *Abbreviations used in this paper*: BFA, brefeldin A; TGN, *trans*-Golgi network; TER, transepithelial resistance.

Materials and Methods

Materials

HRP, type II and VI-A, *o*-dianisidine, *p*-nitrophenyl-*N*-acetyl-β-D-glucosaminide, pronase, diamino-benzidine, BSA (fraction V), SPDP (3-[2 pyridyldithio]-propionic acid *N*-hydroxysuccinimideester), Hepes, and Tris were obtained from Sigma Chemical Co. (St. Louis, MO). Imidazole was obtained from Serva Biochemicals, (Heidelberg, Germany), sucrose from Merck, (Darmstadt, Germany), and BFA from Epicentre Technologies (Madison, WI). The BFA analogues B16 and B21 were a kind gift from Dr. Jennifer Lippincott-Schwartz (National Institutes of Health, Bethesda, MD). Nycodenz was obtained from NYCOMED (Oslo, Norway); [^{3}H]-leucine and Na^{125}I were from the Radiochemical Centre (Amersham, UK). Ricin-HRP conjugates were prepared by the 3-[-2-pyridyldithio]-

propionic acid *N*-hydroxysuccinimideester (SPDP)-method as previously described (38).

Cells

MDCK (strain I), HEp-2, and T47D cells were grown in Costar 3000 flasks (Costar, Badhoevedorp/The Netherlands) or T-25 flasks (NUNC, Roskilde, Denmark). MDCK cells were also seeded on polycarbonate filters (Costar Transwell; pore size, 0.4 μm; diameter, 24.5 mm) at a density of 10^6 per filter and used for experiments 3 or 4 d later (42). Transcytosis of ricin from the basolateral to the apical surface was also determined in MDCK strain II cells. All filters with MDCK I cells used for experiments had a transepithelial resistance of at least 2,000 ohm × cm^2 as measured with the Millicell-ERS equipment (Millipore Corporation, Bedford, MA), also at the end of experiments involving incubation with BFA. The medium used was DME (3.7 g/l sodium bicarbonate; Flow Laboratories, Irvine, Scotland) containing 5% FCS (MDCK) or 10% FCS (HEp-2 and T47D), nonessential amino acids (Gibco, Ltd., Paisley, Scotland) and 2 mM L-glutamine (Gibco, Ltd.). Endocytic uptake measurements of ricin and HRP in MDCK, HEp-2, and T47D cells were performed in Hepes (20 mM) buffered DME with 2 mM glutamine, without sodium bicarbonate (DME-H, Flow Laboratories), supplemented with 0.2% BSA.

Measurement of Cytotoxic Effect

After incubation of MDCK cells on polycarbonate filters with 0–1,000 ng/ml of ricin apically or basolaterally, the medium was removed, and the cells were incubated in the same medium (no unlabeled leucine) for 10 min at 37°C with 1 μCi of [^{3}H]leucine per ml. Then the solution was removed, the cells were washed twice with 5% (wt/vol) TCA and solubilized in KOH (0.1 M). Finally, the acid-precipitable radioactivity was measured. The experiments were carried out in duplicate. The difference between duplicates was <10% of the average value.

Measurement of Endocytosis and Transcytosis of HRP and ^{125}I-Ricin

Endocytosed and transcytosed HRP was quantitated by the *o*-dianisidine reaction as described (3, 43). After endocytic uptake at 37°C cells in 6-well plates or on polycarbonate filters were cooled to 0–4°C and washed 5 × 15 min with cold PBS/0.2% BSA. The cells were subsequently lysed with 1% Triton X-100 and 0.05% SDS, and HRP in the lysate was quantitated. Endocytosis of ^{125}I-labeled ricin (100–200 ng/ml, 30,000–40,000 cpm/ng) was measured as the amount of toxin that could not be removed by 5 × 15 min washes with 0.1 M lactose/0.2% BSA in cold PBS as previously described (30). Transcytosis of ricin was measured as described by van Deurs et al. (42). Incubations with and without BFA were performed as indicated in legends to figures.

Measurement of Ricin Transport to the Trans-Golgi Network by Subcellular Fractionation

Filter-grown MDCK cells were incubated with ^{125}I-ricin (300 ng/ml, 40,000 cpm/ng) apically or basolaterally and washed as described (23). Cells were then scraped off 4–6 filters per experimental point with a rubber policeman after addition of homogenization buffer (H-buffer: 0.3 M sucrose, 3 mM imidazole, pH 7.4). The pooled cells were pelleted by centrifugation for 10 min at 100 *g* and homogenized and fractionated as described (23, 33). Briefly, the postnuclear supernatant (PNS) was subjected to discontinuous gradient centrifugation in a system similar to that reported by Sandberg et al. (29). In the bottom of SW-40 tubes, gradients were made of 4.5 ml light solution (1.15 M sucrose, 15 mM CsCl) and 1.5 ml heavy solution (1.15 M sucrose, 15 mM CsCl, 15% Nycodenz [wt/vol]). The gradients were made in a Biocomp Gradient Master, Nycomed, Oslo (angle 74, speed 16, time 2 min, 45 s). PNS (5.6 parts) was mixed with 2 M sucrose, 10 mM CsCl (4.4 parts), usually a total of 1.5 ml, and layered on top of the gradients. This was again overlayed with 3 ml 0.9 M sucrose, and finally 1–2 ml of 0.3 M sucrose. After 4.5 h at 33,000 rpm in a Beckman SW-40 rotor, the gradients were fractionated (20–28 fractions) and analyzed with respect to marker distribution. The amount of ricin in the Golgi fractions was determined as previously described (23, 33).

Enzyme Analysis

HRP was measured according to Steinman et al. (35), UDP-galactose:glycoprotein galactosyl transferase according to Brändli et al. (4), and β-*N*-acetyl-glucosaminidase according to Beaufay et al. (1).

Electron Microscopy

Filter-grown MDCK cells and near-confluent cultures of MDCK, HEp-2 and T47D cells were rinsed twice with DME-H and incubated with HRP to visualize endosomes and lysosomes in the presence or absence of BFA as follows: In some experiments, cells were incubated with 0, 5, and 20 μg/ml BFA for 30 min at 37°C followed by incubation for 10–60 min at 37°C with the same concentration of BFA and with 5 or 10 mg/ml HRP (Sigma type II). In most cases, the cells were rinsed once at 37°C in DME-H containing BFA in the appropriate concentration, but in some cases this step was repeated several times at 4°C according to the protocol used for biochemical measurements.

In other experiments, cells were pulsed for 30 min at 37°C with 5 or 10 mg/ml HRP in DME-H, rinsed 6 times with DME-H only, and chased for 30 min at 37°C. Then, 0, 5, or 20 μg/ml BFA was added and the cells were incubated for another 30 or 60 min at 37°C and fixed.

In both experimental set-ups, when carried out with filter-grown MDCK cells, BFA was added to both sides of the filter, whereas HRP was added from either the apical or the basolateral side only. Fixation was carried out using either 0.5 or 2% glutaraldehyde in 0.1 M phosphate buffer, pH 7.3, or 2% paraformaldehyde and 0.1% glutaraldehyde in the same buffer. After fixation, cells were processed for DAB-cytochemistry immediately and contrasted en bloc and embedded in Epon as previously described (13). Thin (30–40 nm) and thick (200–400 nm) sections were cut using interference color to monitor section thickness and examined (sometimes after further contrasting with uranyl acetate and lead citrate) in a Jeol 100 CX microscope.

Results

BFA Stimulates Apical Endocytosis in MDCK Cells

Transport of ricin, which binds to galactose residues of membrane glycoproteins and glycolipids, and of the fluid phase marker HRP has been studied extensively in MDCK cells (3, 23, 26, 42, 43). We applied these two markers to study the possible effects of BFA treatment on membrane and fluid transport in confluent MDCK cell monolayers grown on permeable polycarbonate filters. In some experiments the cells were preincubated for 20 min at 37°C with 0–20 μg/ml of BFA, before ricin or HRP was added to the apical or the basolateral medium, followed by another 60 min at 37°C in the presence of BFA. The amount of internalized ricin or HRP was then determined. In the same experiments, transcytosis across the epithelial monolayer was also measured (3, 42).

Cellular accumulation of both ricin and HRP endocytosed from the apical surface was enhanced by BFA concentrations from 2–20 μg/ml, concentrations previously shown to give redistribution of Golgi components to the ER in other cell types than MDCK (6, 10, 17, 18, 24). The increase was ~ twofold for ricin and 2.5-fold for HRP (Fig. 1, *A* and *B*). By contrast, transcytosis in the apical to basolateral direction was largely unaffected (Fig. 1, *C* and *D*).

For our morphological studies we allowed MDCK cells to endocytose HRP for 10–30 min at 37°C, since this allows endosomal compartments to be reached by the tracer, whereas lysosomes only participate to a minor degree (if any) in the overall picture. Moreover, in the short-time experiments (10 min) only early endosomes are reached (3, 26, 42). In the following, all HRP-labeled structures will operationally be referred to as endosomes without any attempt to distinguish earlier from later forms, until we specifically deal with lysosomes. When filter-grown MDCK cells were incubated with

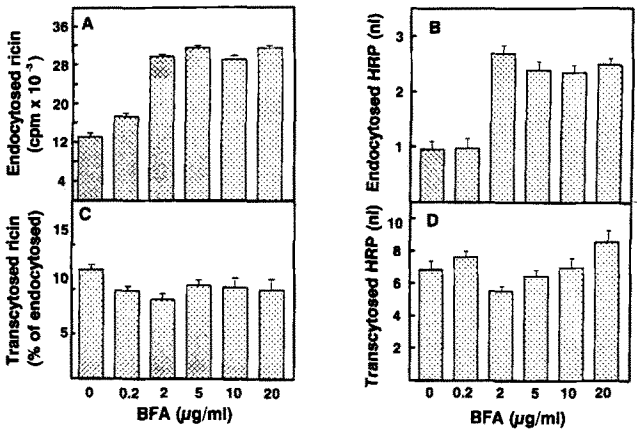

Figure 1. Effect of BFA on apical endocytosis (*A* and *B*) and apical-basolateral transcytosis (*C* and *D*) of ricin (*A* and *C*) and HRP (*B* and *D*). Filter-grown MDCK I cells were preincubated for 20 min at 37°C with concentrations of BFA from 0–20 μg/ml before ^{125}I-ricin (150 ng/ml, 40,000 cpm/mg) or HRP (1 mg/ml) was added to the apical medium. The cells were then incubated for another 60 min, before the filters were transferred to 4°C and washed and analyzed as described in Materials and Methods. The figure shows representative set of three similar experiments with six filters (±SD) per bar.

HRP (5 or 10 mg/ml) from the apical surface for 20 min, followed by fixation, DAB cytochemistry and Epon embedding, light microscopical examination of 2-μm sections cut perpendicular to the filters revealed moderate amounts of labeling in endosomes localized mainly apically (Fig. 2 *a*). When the cells were incubated for 30 min with BFA (5 μg/ml) before addition of HRP to the apical medium and further incubated at 37°C for 10–30 min, we found that ~50% of the cells showed unchanged levels of uptake, compared with the controls. However, in the remaining 50% a dramatic accumulation of HRP-containing apical endocytic structures were seen (Fig. 2 *b*). Analysis of serial sections (1- and 2-μm-thick) in the light microscope clearly revealed that this variation was not within individual cells (e.g., clusters of endocytic vesicles), but were within the population of cells.

To further clarify the kinetics of the increased apical endocytosis in the presence of BFA, we measured the effect of the drug on ricin and HRP uptake during a period of 5–30 min. Increased uptake of both markers could be measured already after 5 min at 37°C (Fig. 3). Since the effect of BFA on apical accumulation of HRP and ricin was rapid, the increased accumulation was most likely caused by a higher endocytic activity at the apical membrane. This view was supported by measurements of the effect of BFA on the recycling of ricin. MDCK cell monolayers were incubated in the presence or absence of BFA (2 μg/ml) for 20 min at 37°C before ^{125}I-ricin was allowed to internalize from the apical or the basolateral side of the filters for 20 min. Membrane-bound ricin was then removed by lactose washes, and recycling was monitored the next 50 min. As shown in Fig. 4, the basolateral recycling of ricin was unchanged, and recycling back to the apical surface domain was only slightly reduced, when expressed as percentage of intracellular ricin after the initial 20 min of internalization.

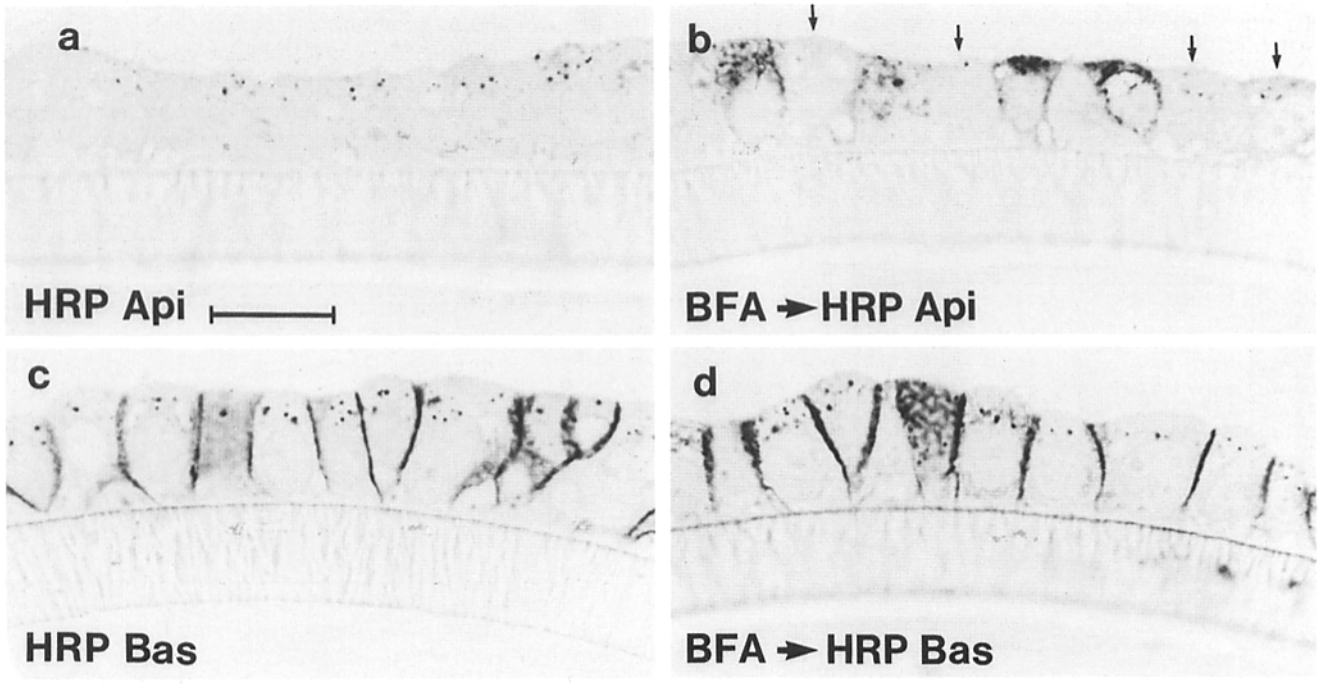

Figure 2. Light micrographs (using a blue filter to enhance the contrast of the brown reaction product) of unstained 2-μm sections of filter-grown MDCK cells exposed to HRP. The specimens were reacted with DAB and embedded in Epon. In *a* the cells were incubated for 20 min at 37°C with HRP (5 mg/ml) from the apical side before a brief wash and fixation. Apical endosomes containing internalized HRP are seen as discrete, dark dots. In *b* the cells were first incubated with BFA (5 μg/ml) for 30 min and then with HRP added apically in the presence of BFA for 20 min at 37°C. Approximately half of the cells show a marked increase in HRP accumulation while the rest (*arrows*) show normal endocytic activity. In *c* the cells have been incubated with HRP added basolaterally for 20 min at 37°C, and in *d*, first with BFA for 30 min and then also with HRP added basolaterally for 20 min. In either case endosomes containing internalized HRP are seen as distinct dots. Thus BFA does not appear to induce increased accumulation from the basolateral surface. Bar, 20 μm.

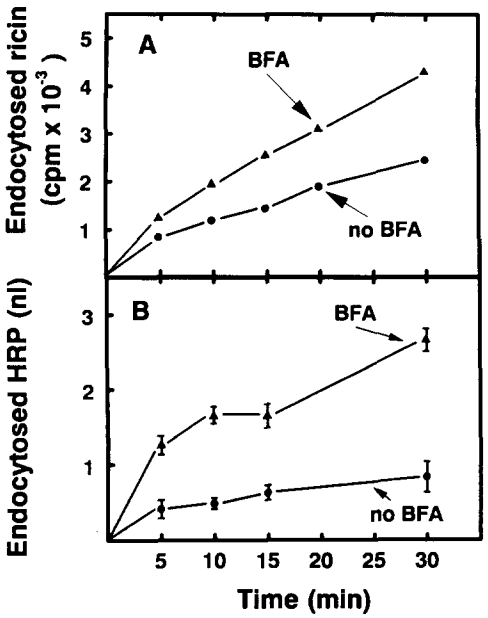

Figure 3. Effect of BFA on apical endocytosis of ricin (*A*) and HRP (*B*) after different times of incubation. Filter-grown MDCK cells were incubated for 20 min at 37°C in the absence or presence of BFA (2 μg/ml), before ^{125}I-ricin (200 ng/ml, 40,000 cpm/ng) or HRP (1.0 mg/ml) was added to the apical medium. The incubations were terminated after the indicated times, and the cells were processed as described in Materials and Methods. Representative sets of three similar experiments. (*A*) Mean of duplicate filters. (*B*) Each value is mean of four filters (±SD).

Since biochemical measurements on BFA-treated MDCK cells thus revealed an overall increase in apical endocytosis of HRP by a factor 2.5, and the light microscopical studies showed a marked heterogeneity in the BFA effect on apical endocytosis, with only 50% of the MDCK cells showing an increase in endocytosis, BFA had actually induced an ~fivefold increase in apical endocytosis of HRP in these cells. The fact that apical fluid phase endocytosis is stimulated more efficiently than membrane endocytosis by BFA, suggests the formation of larger vesicles after BFA treatment.

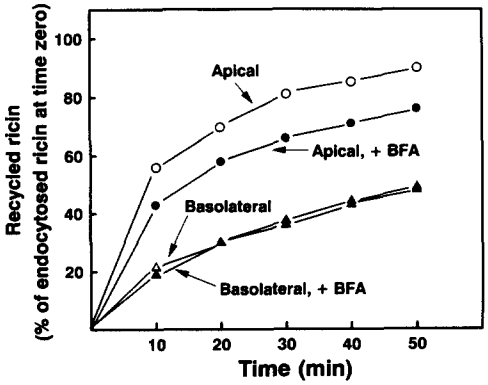

Figure 4. Effect of BFA on recycling of ricin. MDCK monolayers grown on filters were incubated for 20 min at 37°C with or without BFA (2 μg/ml) before ^{125}I-ricin was added to the apical or the basolateral medium. After a loading period of 20 min, cell surface bound ricin was removed with 0.1 M lactose in PBS+ as described in Materials and Methods before recycling of ricin was measured after the indicated times. The medium then contained 10 mM lactose to release recycled cell-surface bound toxin.

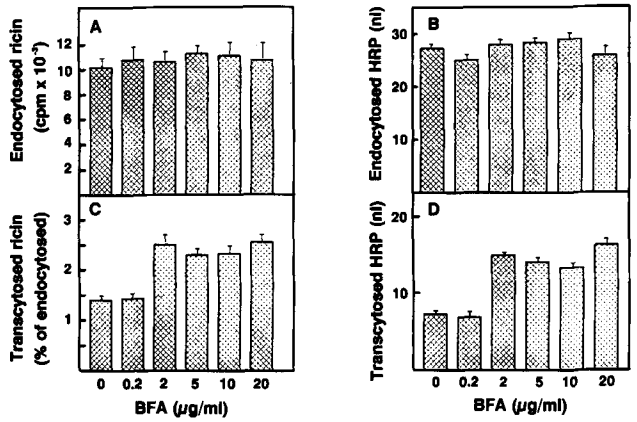

Figure 5. Effect of BFA on basolateral endocytosis (*A* and *B*) basolateral–apical transcytosis (*C* and *D*) of ricin (*A* and *C*) and HRP (*B* and *D*). MDCK cells were preincubated for 20 min at 37°C with BFA (0–20 μg/ml) before ^{125}I-ricin (150 ng/ml, 40,000 cpm/ng) or HRP (0.5 mg/ml) was added to the basolateral medium. The cells were then incubated for another 60 min, before the filters were cooled and processed as described in Materials and Methods. Representative set of three similar experiments. Each bar is mean of six filters (±SD).

Basolateral to Apical Transcytosis Is Stimulated by BFA

Basolateral endocytosis of both ricin and HRP was essentially unchanged in the presence of BFA as revealed by both biochemical and morphological methods (Figs. 2, *c* and *d*, and 5, *A* and *B*). BFA (5 μg/ml) had no effect on the cellular accumulation of HRP and ricin after basolateral administration for shorter periods of time (5, 10, 15 and 30 min, not shown). By contrast, transcytosis from the basolateral to the

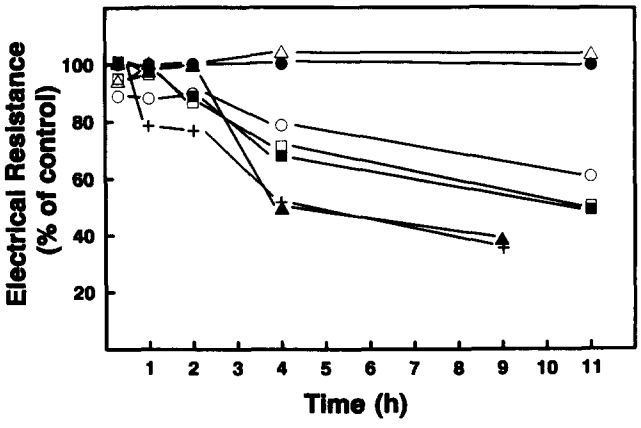

Figure 6. Effect of BFA on the transepithelial resistance of filter-grown MDCK cell monolayers. Filters with confluent MDCK cell monolayers were incubated with 0 (△), 0.5 (●), 1.0 (○), 2.0 (□), 5.0 (■), 10 (▲), or 20 (+) μg/ml BFA for increasing periods of time. TER was measured as described in Materials and Methods. The TER values obtained with the higher concentrations of BFA after 9 or 11 h were still above 1,500 ohm × cm^2. The average TER at time zero was 3,500 ohm × cm^2.

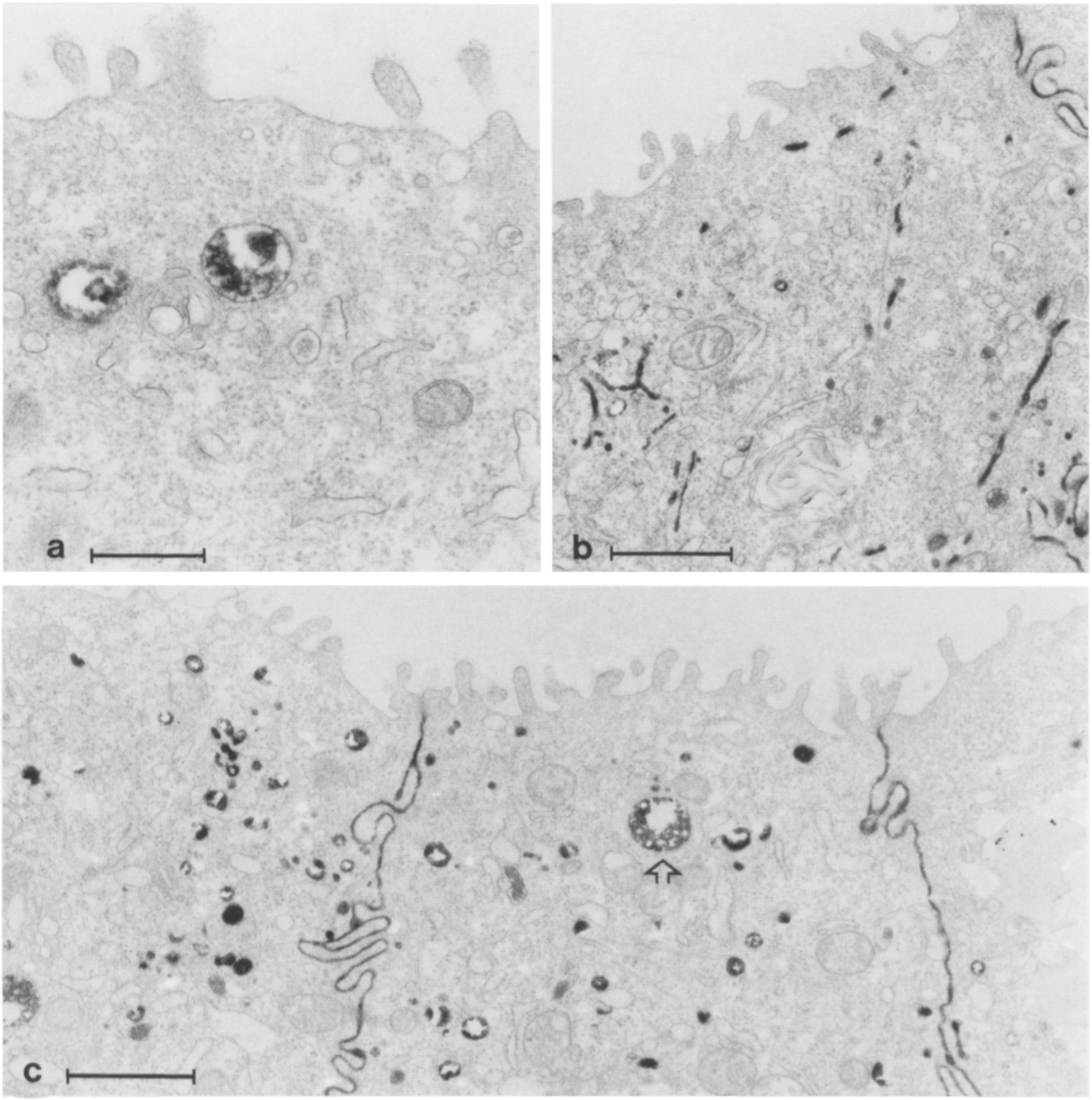

Figure 7. Filter-grown MDCK cells were incubated with BFA (5 μg/ml) for 30 min and thereafter for 20 min with HRP (5 mg/ml) from the basolateral surface in the presence of BFA, before a very brief wash and further processing for EM. In *a* is seen two normal-appearing endosomes of the multivesicular body-type containing HRP, similar to what is found without BFA. In *b*, a cell with distinctly tubular endosomes is shown (as seen in 15–20% of the cell profiles examined), and *c* shows cell profiles with a normal-appearing multivesicular endosome (*arrow*) as well as many smaller, spherical endosomes. Bars: (*a*) 0.5 μm; (*b* and *c*) 1.0 μm.

apical pole of the MDCK cell monolayers was enhanced, 1.5–2-fold for ricin and slightly more for HRP (Fig. 5, *C* and *D*).

To exclude the possibility that BFA caused an opening of tight junctions which would invalidate our measurements of transcytosis, we determined the effect of BFA on the tight junctions by measuring the transepithelial resistance (TER) after treatment of MDCK cell monolayers with BFA (0.5–20.0 μg/ml). BFA induced a reduction in TER between 2 and 4 h after addition of the drug (Fig. 6). After 9 and 11 h the TER had dropped to about half of control values (which were ~3,500 ohm × cm^2 for the filters in Fig. 6), but all endpoint TER values were >1,500 ohm × cm^2. Our endocytosis and transcytosis experiments were all terminated within 2 h from BFA addition.

Since it has recently been shown that BFA inhibits transcytosis of IgA in MDCK II cells transfected with the polymeric IgA receptor (15), we also tested the effect of BFA on basolateral to apical transcytosis of ricin in the MDCK II strain. We found that transcytosis of ricin was stimulated ~twofold both by 2 and 5 μg/ml of BFA also in these cells. In agreement with our results, I. Mellman and co-workers

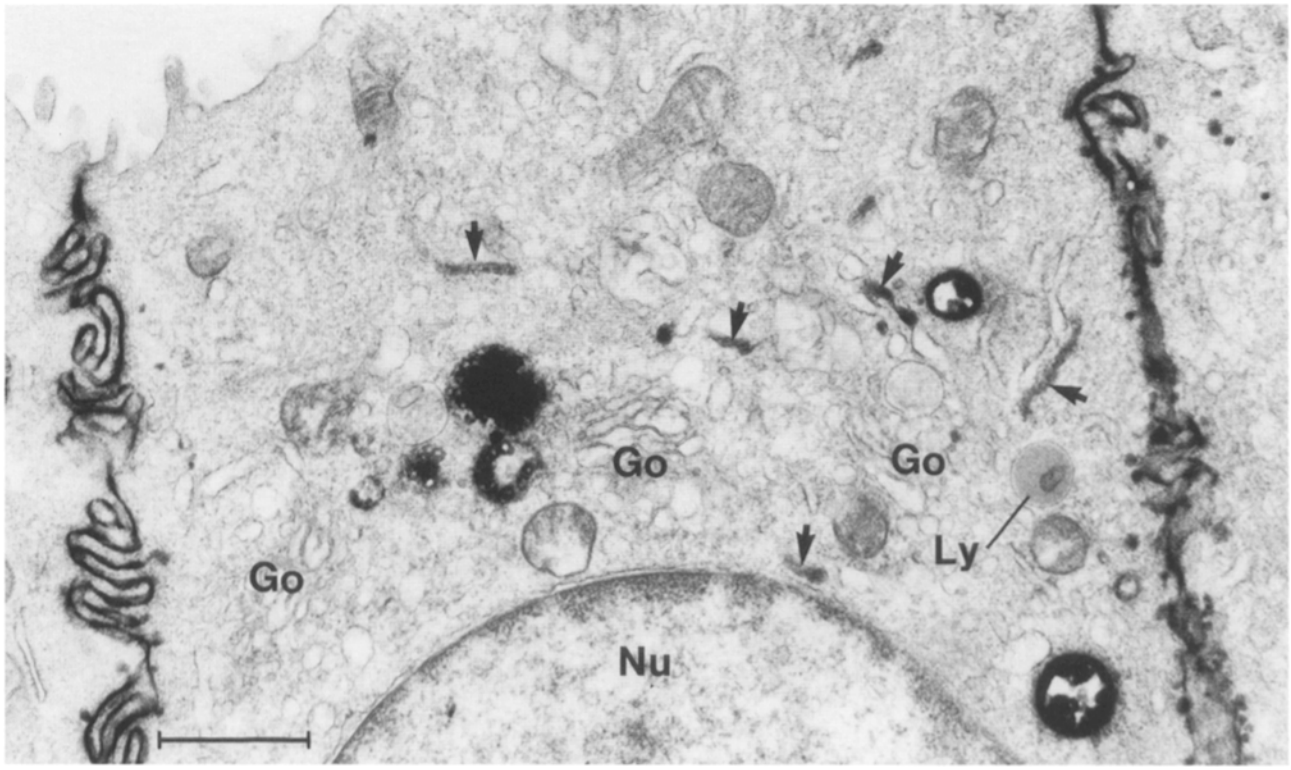

Figure 8. Thick (~250 nm) section of MDCK cells treated as in Fig. 7. Spherical endosomes with HRP are distinct and in addition, some short, tubular endosomes are present (*arrows*). Moreover, a lysosome without HRP (*Ly*) and three Golgi profiles (*Go*) are seen. *Nu*, nucleus. Bar, 1.0 μm.

find that transcytosis of lgp 120 from the basolateral to the apical pole is resistant to BFA under conditions that completely block polymeric IgA (pIgA) transcytosis (I. Mellman, personal communication).

Two BFA analogues, B16 and B21, with very similar molecular structures to BFA, have been shown to be inactive with respect to disruption of the Golgi apparatus (25). These analogues could neither stimulate apical endocytosis, nor basolateral–apical transcytosis in MDCK cells (not shown).

Ultrastructural Analysis of Endosomes and Lysosomes in BFA-treated Cells

We next analyzed ultrastructurally the effect of BFA on internalization of HRP in polarized MDCK cells. In most of the morphological studies, very short washes were used at 37°C before fixation to interfere as little as possible with cell structure. Therefore HRP was mostly present in the intracellular spaces after basolateral administration (Fig. 7 and 8). With the thorough washing procedure at 4°C in the quantitative biochemistry part of the studies reported here, a complete washout of HRP was observed.

In control cells, endocytosis of HRP from the basolateral surface for 10–30 min at 37°C mainly gave rise to spherical (sometimes multivesicular) endosomes in the lateral and apical cytoplasm. It is well established that the endosomal system of various cell types comprises both vacuolar and tubulo-vesicular portions (11, 21, 37, 39), and this is also true for the MDCK cells, although endosomal tubules were rather sparse as revealed by examination of thin (30–40 nm) as well as thick (200–400 nm) sections.

When MDCK cells were incubated with BFA (5 μg/ml) for 20–30 min before incubation with HRP at the basolateral side for 10–30 min, some endosomes were clearly tubular (tubule diameter of 50–100 nm), in agreement with recent studies on NRK cells (19) as well as MDCK cells (15). This was distinct in ~15–20% of the cell profiles examined (Fig. 7 *b*). In addition, many small vesicles (diameter range 50–300 nm) were observed in some cells (Fig. 7 *c*). The spherical nature of these structures was settled by using thick sections and thin serial sections. These small vesicles were more frequent after BFA treatment than in control cells (see Fig. 12 *B*) and may therefore, in addition to endosomal tubules, be induced by BFA. Finally, normal-appearing (spherical) endosomes (diameter range 0.3–0.6 μm) were seen in most cells (Figs. 7 and 8).

In control cells, endocytosis of HRP from the apical surface for 10–30 min was rather limited, and typically gave rise to 1–5 spherical endosomes per cell profile, 0.3–0.6 μm in diameter (see Fig. 12 *A*) and sometimes with the appearance of multivesicular bodies. In addition, some small (50–300 nm) vesicles and a few endosomal tubules were noticed. This is in agreement with previous reports that cellular accumulation of HRP after endocytosis from the apical surface is less than from the basolateral surface of MDCK cells, where the basolateral surface area is at least threefold larger than the apical surface area (3, 26, 43).

When the cells were treated with BFA (5 μg/ml) for 30 min before exposure to HRP for 10–30 min from the apical surface, the marker was found in large amounts of vesicles and tubules, clearly reflecting the marked BFA-induced increase

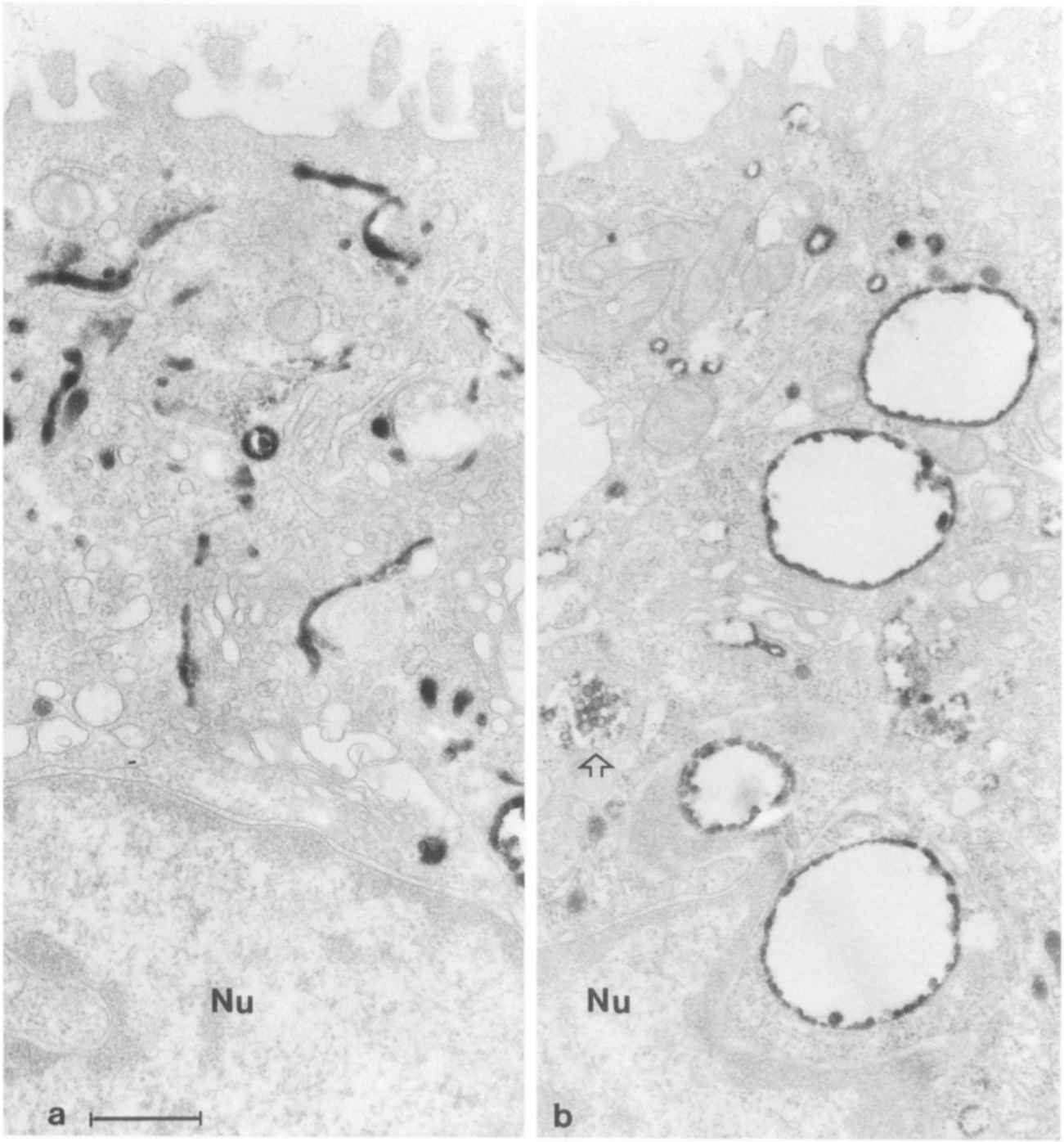

Figure 9. Filter-grown MDCK cells were incubated for 30 min with BFA (5 μg/ml) followed by 20 min with HRP (5 mg/ml) from the apical surface in the presence of BFA. *a* shows numerous tubular endosomes as seen in ~20% of the cells, and in *b* four large endosome vacuoles are shown, representing the situation in other 30–50% of the cells. The arrow in *b* indicates a normal-sized multivesicular endosome. *Nu*, nucleus. Bar, 0.5 μm.

in endocytosis of HRP from the apical surface as revealed biochemically. Already after 10 min of HRP incubation, cells with tubular endosomes were found and after 20 min ~20% of all cell profiles contained elaborate systems of 50–100-nm wide tubular structures with HRP as shown in Fig. 9 *a*. Even though single tubules could be followed for up to 2–3 μm, especially in thick sections, the tubular systems often comprised aligned, shorter tubular endosomes and endosomal vesicles of varying size (Fig. 10). Tubules were frequently connected to endosomal vesicles and the aligned vesicles and tubules were often associated with parallel microtubules (Fig. 10, *d* and *e*). In addition, the apical cytoplasm of other 30–50% of the cell profiles contained large numbers of HRP-labeled spherical endocytic structures, sometimes almost completely occupying the cytoplasm (Figs. 9 *b* and 11, *c* and *d*). This was clearly different from what was seen after basolateral endocytosis in BFA-treated cells. The spherical shape of these numerous BFA-induced

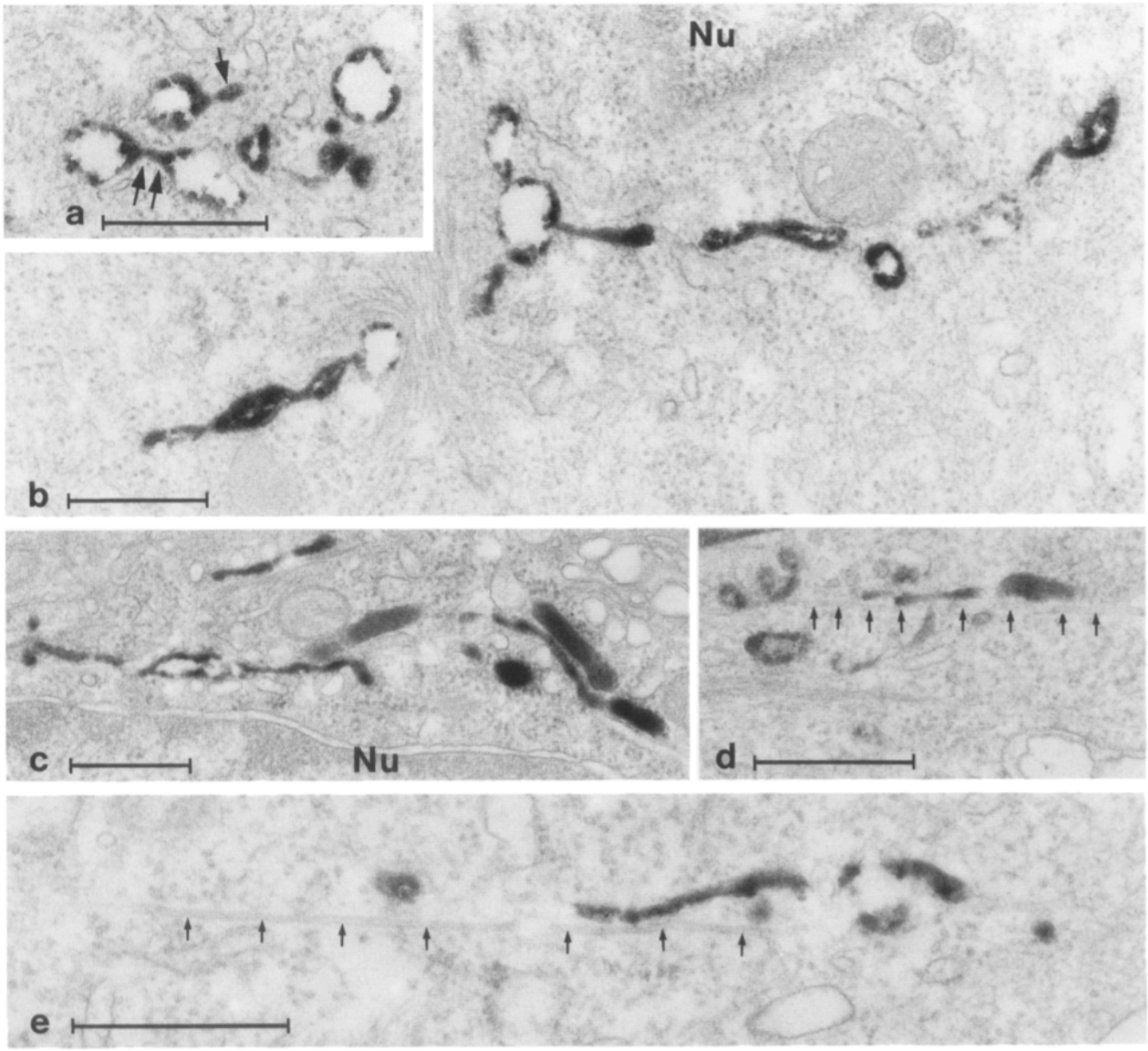

Figure 10. Examples of endosome tubulation. Filter-grown MDCK cells were incubated for 30 min with BFA (5 μg/ml) followed by 10–30 min with BFA plus HRP (5 mg/ml) from the apical side. In *a* a short tubular process is shown emerging from a spherical endosome (*arrow*) as well as two spherical endosomes connected by a tubular bridge (*double arrow*), and in *b* and *c* aligned spherical and tubular endosomes are shown. These aligned endosomal elements are often associated with parallel bundles of microtubules as shown in *d* and *e* (*arrows*). *Nu*, Nucleus. Bars, 0.5 μm.

vesicles and vacuoles was established using thin and thick consecutive sections. The diameter distribution of these structures is shown in Fig. 12 *A*. It is obvious that BFA has induced both myriads of small vesicles (0–300 nm) as well as fewer, but much larger, vacuoles (700–1,300 nm), as compared with the situation without BFA. These larger (>700 nm) vacuoles (Fig. 9 *b*), however, contain severalfold more fluid than the small (<300 nm) vesicles and can readily ac-

Figure 11. a–d are examples of spherical endosomes after treatment of filter-grown MDCK cells as described for Fig. 10. *a* shows a portion of the apical cytoplasm with a single, multivesicular endosome (*open arrow*) and a short tubular endosome above (*small arrow*), a situation similar to that found in control cells. A lysosome (*Ly*) and two Golgi complexes (*Go*) without HRP are also seen. *b* shows two multivesicular endosomes (*arrows*) surrounded by smaller endosomal vesicles, and *c* shows numerous spherical endosomes of various size. *d* shows a thick (~250 nm) section through a cell similar to that shown in *c*. *e* and *f* are from experiments, where the filter-grown MDCK cells first were pulsed for 30 min with HRP (5 mg/ml) from the apical surface, then washed carefully and further chased for 30 min before the cells were incubated for 60 min with BFA (5 μg/ml). Two spherical lysosomes (*Ly*) containing HRP are shown. In addition, an unlabeled tubular endosome (*small arrows* in *e*) and some spherical endosomes (*arrows* in *f*) are seen. Bars, 0.5 μm.

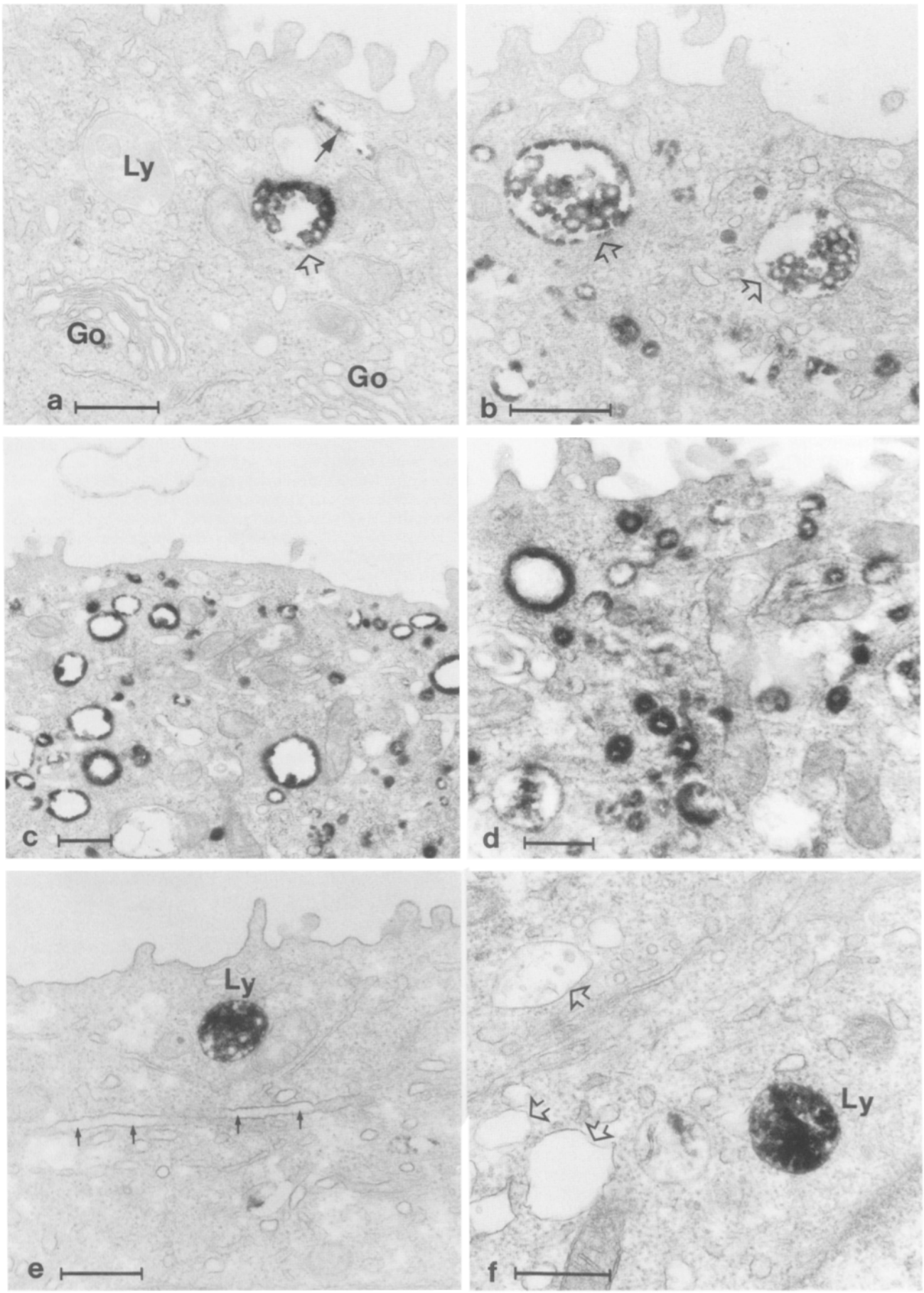
Ly
Go
Go
a
b
c
d
Ly
e
Ly
f

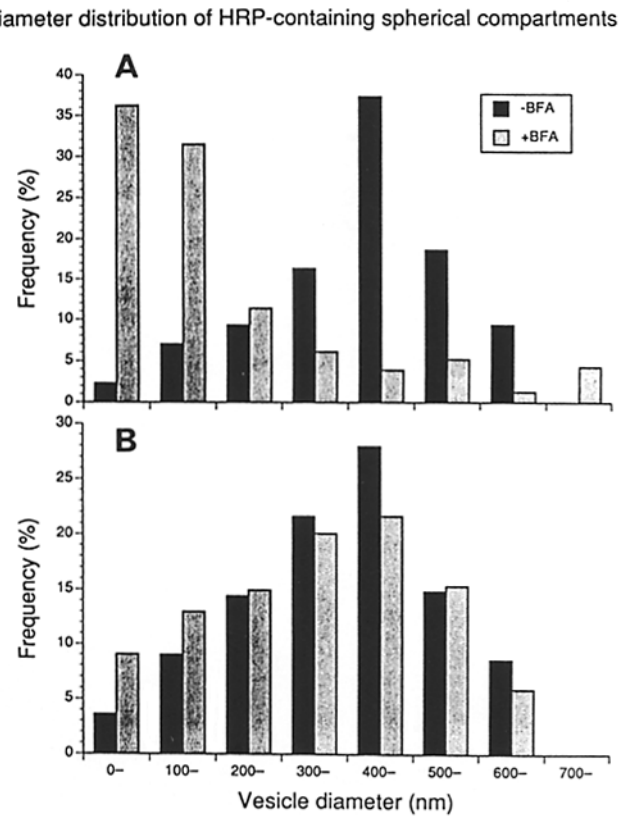

Figure 12. Diameter distribution of HRP-containing spherical compartments after apical (*A*) and basolateral (*B*) administration of HRP. Filter-grown MDCK cells were incubated for 20 min with HRP (5 mg/ml) (■) or for 30 min with BFA (5 μg/ml) followed by 20 min with HRP in the presence of BFA (▨) from the apical or the basolateral side. The diameter of vesicles was measured in randomly photographed cell profiles not showing distinct endosome tubulation (as shown in Fig. 7 *b* and 9 *a*). It is seen that after BFA treatment, both numerous small and some very large spherical endosomes have been generated selectively from the apical surface.

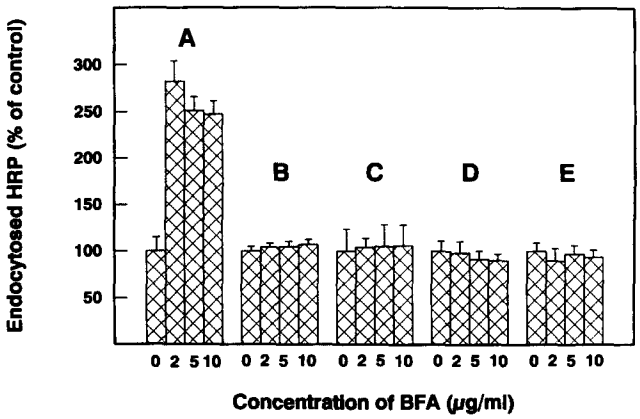

Figure 13. Effect of BFA (0, 2, 5, and 10 μg/ml) on fluid phase endocytosis in filter-grown MDCK cells (apical [*A*] or basolateral [*B*] administration), subconfluent MDCK cells (*C*), HEp-2 cells (*D*), and T47D cells (*E*) grown in 6-well plastic dishes. Cells were treated with the indicated concentrations of BFA for 20 min at 37°C, before HRP was added and the incubations proceeded for another 60 min. The cells were subsequently cooled to 4°C and the cells on filters or in 6-well plates were washed five times, 15 min each (with shaking) in ice-cold PBS/0.2% BSA, before HRP accumulation within the cells was measured. In parallel experiments the preincubation with BFA was performed at 37°C, while the incubation with HRP was carried out at 4°C. Only negligible amounts of cell associated HRP could be detected after the washing procedure, and these background values were subtracted from those obtained at 37°C. The figure shows a representative set of bars from one of at least three similar experiments in each category. Bars represent mean of six experimental values (±SD).

count for the increase in HRP uptake from the apical surface after BFA treatment. In the remaining cell profiles, that is, in those without the pronounced increase in number of HRP-labeled vesicles, a few (1–5) spherical endosomes (0.3–0.6 μm in diameter) were present, presumably corresponding to the endosomes also found in the cells not exposed to BFA (Fig. 11, *a* and *b*). The fact that the examined cell profiles often contained either a few normally appearing endosomes (Fig. 11, *a* and *b*), or tubular endosomes (Fig. 9 *a*), or most frequently, large amounts of spherical endosomal vesicles of various sizes (Figs. 9 *b* and 11, *c* and *d*), suggests a heterogeneity in the endosomal populations of MDCK cells, at least in relation to the effect of BFA.

When the MDCK cells were pulse chased with HRP from either the apical or the basolateral surface for 30 + 30 min at 37°C followed by 60 min with BFA, the tracer was clearly confined to spherical structures operationally defined as lysosomes (Fig. 11, *e* and *f*). However, empty (nonHRP-labeled) tubules and vacuoles of various sizes in the apical cytoplasm were noticed (Fig. 11, *e* and *f*). The round shape of lysosomes was emphasized using thick sections. Accordingly, we found no BFA-induced changes in the morphology of lysosomes in MDCK cells, in contrast to what has recently been reported for NRK cells (19).

To further document the selective, BFA-induced increase in apical endocytosis in polarized MDCK cells and concomitant formation of frequent, spherical endocytic vesicles and vacuoles, we next examined the effect of BFA on endocytosis and endosome morphology in HEp-2, T47D, and MDCK cells grown on plastic. Even though HEp-2 cells develop some degree of polarity, this is definitely less than what can be obtained with MDCK cells. T47D cells do not develop tight junctions and membrane polarity (40). Moreover, we have extensive knowledge on the effects of BFA on the Golgi apparatus of these cell lines. Thus, BFA transforms Golgi stacks of HEp-2 and T47D cells into characteristic tubulovesicular Golgi reticula (32), which were used in the present study as an "internal" control that BFA had actually influenced the cells (not shown).

As found for endocytosis from the basolateral surface of filter-grown MDCK cells, BFA had no effect on endocytosis of HRP in HEp-2, T47D and subconfluent MDCK cells grown on plastic (Fig. 13). BFA did stimulate to some extent cellular accumulation of HRP in highly confluent MDCK cells grown on plastic (not shown). Under these conditions the plasma membrane facing the medium bears resemblance to the apical membrane of truly polarized MDCK cells (22).

EM revealed spherical endosomes as well as tubular endosomes containing HRP in the three cell lines on plastic. When the cells were exposed to BFA for 30 min before incubation with HRP for 10–60 min at 37°C, spherical endosomes were clearly predominating even in thick sections (Fig. 14 *a*), although tubulation could be rather pronounced regionally (Fig. 14 *b*). It should be stressed that tubular endosomes identical to those shown in Fig. 14 *b* could be

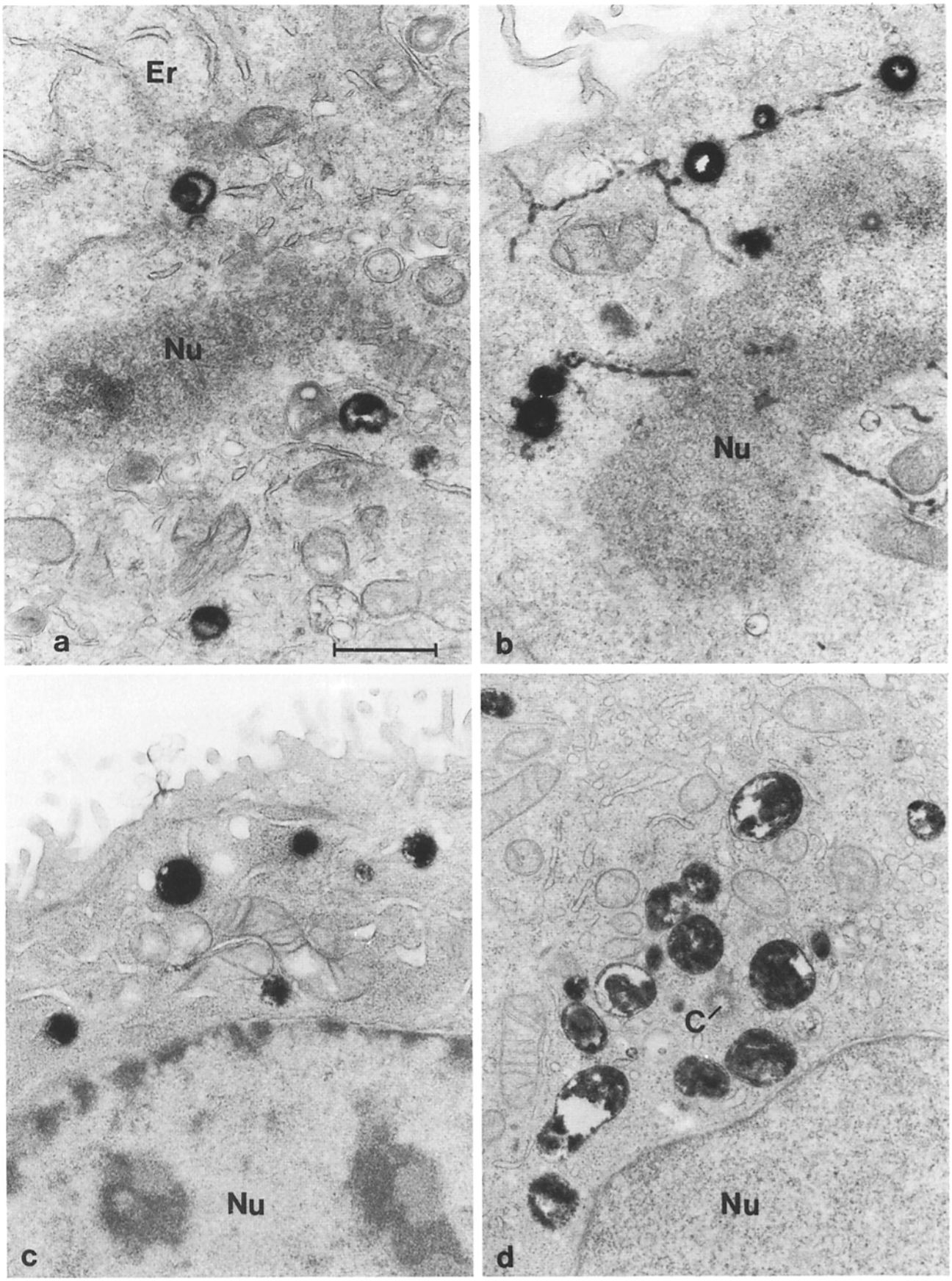

Figure 14. (*a* and *b*) Thick (200 nm) sections of HEp-2 cells grown on plastic and incubated with BFA (20 μg/ml) for 30 min and thereafter for 30 min with HRP (10 mg/ml) in the presence of BFA. While in most cases little or no endosome tubulation was observed (*a*), a distinct tubulation was sometimes seen (*b*). *Er*, endoplasmic reticulum; *Nu*, nucleus (in both micrographs sectioned tangentially; nuclear pores may be seen). *c* is a thick (200 nm) and *d* a thin section of HEp-2 cells which were first pulsed for 30 min with HRP (10 mg/ml), then washed and further chased for 30 min before the cells were incubated for 60 min with BFA (20 μg/ml). The resulting HRP-labeled lysosomes are distinctly spherical. *Nu*, nucleus. C (in *d*) is a centriole. Bars, 1.0 μm.

found, although less frequently, in control cells as well, in particular in thick sections (36).

In experiments with HRP designed to label lysosomes of HEp-2 and T47D cells (see above) before addition of BFA, no HRP-labeled tubules were noticed. Thus, as for MDCK cells we found that lysosomes were distinctly spherical also after BFA treatment (Fig. 14 *c* and *d*).

Since the experimental and further preparative procedure may influence the final result in the electron microscope with respect to vacuolar versus tubular endosomes (36), we used (*a*) both 5 and 20 μg/ml BFA, and (*b*) both 5 and 10 mg/ml HRP (Sigma type II). Irrespective of the amount of HRP used, the following DAB cytochemistry was always carried out immediately after fixation and lasted for 30 min (routine procedure in our previous studies as well). Moreover, we used (*c*) different fixatives: 2% glutaraldehyde, 0.5% glutaraldehyde, or 0.1% glutaraldehyde + 2% formaldehyde and (*d*) fixations at both 4, 20–22, and 37°C. However, neither of these procedures (*a–d*) modified what we saw in the electron microscope. Finally, as already described (*e*) both thin (30–40 nm) and thick (200–400 nm) sections were examined in the electron microscope.

MDCK Cells Are Sensitized to Ricin by BFA

While BFA protects most cell lines against ricin, BFA actually sensitized MDCK cells grown on plastic to the toxin (32). Moreover, as reported previously (15, 32) and also confirmed here, BFA does not change Golgi morphology in MDCK cells (data not shown). In relation to ricin this is interesting since transport of internalized ricin to the Golgi complex seems to be important for the toxic effect (31, 38, 41). We next investigated if BFA would sensitize the cells to ricin both after apical and basolateral addition of the toxin. BFA did actually increase the toxicity of ricin in both cases (not shown). The amount of ricin transported to the Golgi apparatus was therefore measured by subcellular fractionation (Table I). The transport from the apical side seemed to be slightly increased (expressed as percent of internalized ricin), while from the basolateral side, there was a small reduction in ricin transport to the Golgi fractions in the presence of BFA. Thus, other phenomena than increased transport to the Golgi apparatus seem to be responsible for the increased toxicity of ricin. Cycloheximide has previously been shown to sensitize other cell lines to ricin (31), and also MDCK cells were sensitized to the toxin by cycloheximide. A combination of BFA and cycloheximide did not give any further sensitization (data not shown), indicating that similar mechanisms may be responsible for this effect of these drugs.

Discussion

In this study, we have examined the effect of the isoprenoid fungal product BFA on membrane and fluid transport after endocytic uptake of ricin and HRP in polarized MDCK epithelial cells.

Two transport routes were highly stimulated by BFA, the apical endocytic uptake and transcytosis in the basolateral to apical direction. None of the studied transport routes seemed to be dramatically blocked, but we found some reduction in the transport of ricin to the Golgi apparatus.

Effect of BFA on Apical Endocytosis

Endocytosis from the apical surface of MDCK cells is the first example of a vesicular transport route that is stimulated by BFA. The uptake of both the membrane marker ricin and the fluid phase marker HRP was stimulated twofold or more. It has been shown recently that BFA treatment causes tubulation of endosomes (15, 19). In the present study we also find endosome tubulation, but it should be stressed that a marked heterogeneity in endosome response to BFA exists in all cell types here examined (MDCK, HEp-2, T47D), and that spherical shapes are still predominating in the total endosome population at the ultrastructural level, irrespective of the experimental setup and subsequent preparative procedures. More or less extended tubular or tubulo-vesicular endosomes or endosome processes associated with spherical endosomes have been described in several cell types and by various approaches (11, 14, 21, 36, 37, 39). One could therefore speculate that tubular and spherical endosomal elements exist in a dynamic equilibrium and that this equilibrium is dependent on cell type (cell line), physiological, and presumably also experimental conditions. After BFA treatment it is shifted towards more tubules. Thus, in individual random sections or micrographs, tubular endosomes of identical appearance can be seen both in control cells and in cells treated with BFA. It is therefore interesting that the increased endocytosis observed specifically from the apical surface of filter-grown MDCK cells after BFA treatment apparently involved de novo formation of numerous spherical endosomes of various sizes, rather than appearance of more frequent tubular endosomes as seen also in other cell types (e.g., HEp-2 and T47D), where BFA does not increase endocytosis.

Apical and basolateral endocytosis in MDCK cells is known to involve distinct sets of apical and basolateral early endosomes (3, 26). These two classes of endosomes sort internalized markers differently (3), and are unable to ex-

Table I. Effect of BFA on Internalization of ^{125}I-Ricin and Transport of the Toxin to the Golgi Fractions in MDCK Cells

Side of administration		Internalized ricin	Ricin in the Golgi fractions (in percent of internalized ricin)
		cpm	
Apical	+BFA	$1.90 \times 10^6 \pm 0.13 \times 10^6$	4.5 ± 0.4 ($n = 5$)
Apical	−BFA	$1.13 \times 10^6 \pm 0.09 \times 10^6$	3.6 ± 0.5 ($n = 5$)
Basolateral	+BFA	$7.14 \times 10^6 \pm 0.16 \times 10^6$	3.5 ± 0.1 ($n = 3$)
Basolateral	−BFA	$7.55 \times 10^6 \pm 0.21 \times 10^6$	5.2 ± 0.2 ($n = 3$)

After preincubation with or without BFA for 20 min at 37°C, ^{125}I-ricin was added to the apical or the basolateral medium (300 ng/ml, 40,000 cpm/ng). The incubation was continued for 60 min at 37°C. Homogenization and subcellular fractionation was carried out as described in Materials and Methods. The amounts of ricin in the Golgi fractions are given as the mean of 3–5 experiments ± SD.

change content by in vitro fusion (2). The fact that BFA only stimulates apical endocytosis in MDCK cells is another argument for the existence of important functional differences in the apical and the basolateral endocytic pathways in MDCK cells. The underlying mechanism for the stimulation of apical endocytosis by BFA is not evident. Although BFA treatment of most cell types has dramatic consequences for the morphology of the Golgi apparatus and also results in changes in the appearance of the early endosomal compartment and the TGN (15, 19, 28, 44), the functional consequences of BFA treatment are less well known. The return of the Golgi stacks to the ER results in a block in protein secretion (24). The microtubule-dependent tubulation of early endosomes (15, 19, 44) and changes in TGN morphology (19, 44) seen with BFA have been suggested to be accompanied by colocalization of labeled early endosomes with TGN markers, presumably by fusion of the two compartments (19, 44). The earliest events detected after addition of BFA to cells is the dissociation of coat proteins from the Golgi complex resulting in a cytosolic distribution pattern (7, 9, 34). It has been proposed that one important role of coat structures is to prevent the interaction of membrane buds with microtubules by packing in the microtubule motor proteins, and that the morphological results of BFA treatment is due to the rapid dissociation of coat structures (27). This hypothesis is supported by the order of events of the changes the Golgi apparatus undergoes with BFA treatment. Likewise, it is possible that the BFA-stimulated increase in apical endocytosis is due to dissociation of certain proteins from the apical membrane, proteins that serve to regulate the rate of endocytosis.

Effect of BFA on Basolateral to Apical Transcytosis

We found that, in addition to apical endocytosis, the basolateral to apical transcytosis of ricin and HRP was also stimulated by BFA treatment. In contrast, transcytosis of pIgA was found to be blocked by BFA treatment (15). These apparently different results are not due to MDCK cell clonal variance. In agreement with this, transcytosis of lgp 120 is resistant to concentrations of BFA that block pIgA transcytosis (I. Mellman, personal communication). Indirect lines of evidence indicated that the pIgA receptor was unable to exit from early basolateral endosomes. This effect could be due to the dissociation of a cytoplasmic coat of yet unknown composition from early endosomes (15). Our finding that transcytosis of general membrane and fluid phase markers like ricin and HRP is not blocked by BFA, but rather enhanced in the basolateral-apical direction could be explained by different models. One possibility is that BFA disturbs the proper association of the pIgA receptor with transcytotic vesicles budding from early basolateral endosomes. Another possibility could be that there are two or more transcytotic pathways working in parallel, and that one of these, responsible for the transcytosis of pIgA is blocked. This would imply that more than one type of transcytotic vesicle buds off from early basolateral endosomes.

Possible Effects of BFA on the Golgi Apparatus in MDCK Cells

MDCK cells and PtK cells are the two cell lines discovered until now with Golgi stacks that seem morphologically resistant to BFA (15, 16, 32). However, although no morphologi cal changes have been detected in the Golgi apparatus o MDCK cells during BFA treatment, several processes in volving the Golgi apparatus are affected. Apical protein secretion is inhibited by low concentrations of BFA (20). The inhibited step could be at the level of the TGN, where apica and basolateral components are sorted into vesicles destinec for the apical and basolateral surfaces, respectively (12). The intoxication of cells by ricin is believed to involve endocytosis and transport to the TGN followed by translocation from the TGN or a nearby compartment (41). While BFA protected most cell lines against ricin (32), MDCK cells actually became more sensitive after both apical and basolateral administration of the toxin. This could, at least for uptake of ricin from the basolateral surface, not be explained by increased transport of ricin to the Golgi apparatus. Thus it is possible that BFA has an effect on the Golgi apparatus of MDCK cells, although this organelle seems unaffected structurally.

We thank Dr. J. Lippincott-Schwartz for generously providing the BFA analogues B16 and B21. We are grateful to Anne-Grethe Myrann, Anne Thorp, Tove Lie Berle, Jorunn Jacobsen, Marianne Lund, Keld Ottosen, and Kirsten Pedersen for expert technical assistance.

This work was supported by the Norwegian Research Council for Science and the Humanities (NAVF), The Norwegian Cancer Society, The Danish Cancer Society, The Danish Medical Research Council, the NOVO Foundation, the P. Carl Petersen Foundation, the Wedellsborg Foundation, and NATO Collaborative Research Grant (CRG 900517).

Received for publication 23 March 1992 and in revised form 27 May 1992.

References

1. Beufay, H., A. Amar-Costesec, E. Feytmans, A. Thinès-Sempoux, M. Wibo, M. Robbi, and J. Berthet. 1974. Analytical study of microsomes and isolated subcellular membranes from rat liver. I. Biochemical methods. *J. Cell Biol.* 61:188–200.
2. Bomsel, M., R. Parton, S. A. Kuznetsov, T. A. Schroer, and J. Gruenberg. 1990. Microtubule- and motor-dependent fusion in vitro between apical and basolateral endocytic vesicles from MDCK cells. *Cell.* 62:719–731.
3. Bomsel, M., K. Prydz, R. G. Parton, J. Gruenberg, and K. Simons. 1989. Endocytosis in filter-grown Madin-Darby canine kidney cells. *J. Cell Biol.* 109:3243–3258.
4. Brändli, A. W., G. C. Hansson, E. Rodriguez-Boulan, and K. Simons. 1988. A polarized epithelial cell mutant deficient in translocation of UDP-galactose into the Golgi complex. *J. Biol. Chem.* 263:16283–16290.
5. Chege, N. W., and S. R. Pfeffer. 1990. Compartmentalization of the Golgi complex: Brefeldin A distinguishes *trans*-Golgi cisternae from the *trans*-Golgi network. *J. Cell Biol.* 111:893–899.
6. Doms, R. W., G. Russ, and J. W. Yewdell. 1989. Brefeldin A redistributes resident and itinerant Golgi proteins to the endoplasmic reticulum. *J. Cell Biol.* 109:61–72.
7. Donaldson, J. G., J. Lippincott-Schwartz, G. S. Bloom, T. E. Kreis, and R. D. Klausner. 1990. Dissociation of a 110-kD peripheral membrane protein from the Golgi apparatus is an early event in brefeldin A action. *J. Cell Biol.* 111:2295–2306.
8. Donaldson, J. G., R. A. Kahn, J. Lippincott-Schwartz, and R. D. Klausner. 1991. Binding of ARF and β-COP to Golgi membranes: Possible regulation by a trimeric G protein. *Science (Wash. DC).* 254:1197–1199.
9. Duden, R., G. Griffiths, R. Frank, P. Argos, and T. E. Kreis. 1991. β-COP, a 110 kd protein associated with non-clathrin-coated vesicles and the Golgi complex, shows homology to β-adaptin. *Cell.* 64:649–665.
10. Fujiwara, T., K. Oda, S. Yokota, A. Takatsuki, and Y. Ikehara. 1988. Brefeldin A causes disassembly of the Golgi complex and accumulation of secretory proteins in the endoplasmic reticulum. *J. Biol. Chem.* 263:18545–18552.
11. Geuze, H. J., J. W. Slot, G. J. A. M. Strous, H. F. Lodish, and A. L. Schwartz. 1983. Intracellular site of asialoglycoprotein receptor-ligand uncoupling: Double-label immunoelectron microscopy during receptor-mediated endocytosis. *Cell.* 32:277–287.
12. Griffiths, G., and K. Simons. 1986. The trans Golgi network: Sorting at the exit site of the Golgi complex. *Science (Wash. DC).* 234:438–443.
13. Hansen, S. H., K. Sandvig, and B. van Deurs. 1991. The preendosomal compartment comprises distinct coated and noncoated endocytic vesicle

populations. *J. Cell Biol.* 113:731–741.
14. Hopkins, C. R., A. Gibson, M. Shipman, and K. Miller. 1990. Movement of internalized ligand-receptor complexes along a continuous endosomal reticulum. *Nature (Lond.).* 346:335–339.
15. Hunziker, W., J. A. Whitney, and I. Mellman. 1991. Selective inhibition of transcytosis by brefeldin A in MDCK cells. *Cell.* 67:617–627.
16. Ktistakis, N. T., M. G. Roth, and G. S. Bloom. 1991. PtK1 cells contain a nondiffusible, dominant factor that makes the Golgi apparatus resistant to brefeldin A. *J. Cell Biol.* 113:1009–1023.
17. Lippincott-Schwartz, J., L. C. Yuan, J. S. Bonifacino, and R. D. Klausner. 1989. Rapid redistribution of Golgi proteins into the ER in cells treated with Brefeldin A: Evidence for membrane cycling from Golgi to ER. *Cell.* 56:801–813.
18. Lippincott-Schwartz, J., J. G. Donaldson, A. Schweizer, E. G. Berger, H.-P. Hauri, L. C. Yuan, and R. D. Klausner. 1990. Microtubule-dependent retrograde transport of proteins into the ER in the presence of Brefeldin A suggests an ER recycling pathway. *Cell.* 60:821–836.
19. Lippincott-Schwartz, J., L. Yuan, C. Tipper, M. Amherdt, L. Orci, and R. D. Klausner. 1991. Brefeldin A's effects on endosomes, lysosomes, and the TGN suggests a general mechanism for regulating organelle structure and membrane traffic. *Cell.* 67:601–616.
20. Low, S. H., S. H. Wong, B. L. Tang, P. Tan, V. N. Subramaniam, and W. Hong. 1991. Inhibition by brefeldin A of protein secretion from the apical cell surface of Madin-Darby canine kidney cells. *J. Biol. Chem.* 266:17729–17732.
21. Marsh, M., G. Griffiths, G. E. Dean, I. Mellman, and A. Helenius. 1986. Three-dimensional structure of endosomes in BHK-21 cells. *Proc. Natl. Acad. Sci. USA.* 83:2899–2903.
22. Matlin, K., D. F. Bainton, M. Pesonen, D. Louvard, N. Genty, and K. Simons. 1983. Transepithelial transport of a viral membrane glycoprotein implanted into the apical plasma membrane of Madin-Darby canine kidney cells. I. Morphological evidence. *J. Cell Biol.* 97:627–637.
23. Melby, E. L., K. Prydz, S. Olsnes, and K. Sandvig. 1991. Effect of monensin on ricin and fluid phase transport in polarized MDCK cells. *J. Cell Biochem.* 47:1–10.
24. Misumi, Y., K. Miki, A. Takatsuki, G. Tamura, and Y. Ikehara. 1986. Novel blockade by Brefeldin A of intracellular transport of secretory proteins in cultured rat hepatocytes. *J. Biol. Chem.* 261:11398–11403.
25. Orci, L., M. Tagaya, M. Amherdt, A. Perrelet, J. G. Donaldson, J. Lippincott-Schwartz, R. D. Klausner, and J. E. Rothman. 1991. Brefeldin A, a drug that blocks secretion, prevents the assembly of non-clathrin-coated buds on Golgi cisternae. *Cell.* 64:1183–1195.
26. Parton, R. G., K. Prydz, M. Bomsel, K. Simons, and G. Griffiths. 1989. Meeting of the apical and basolateral endocytic pathways of the Madin-Darby canine kidney cell in late endosomes. *J. Cell Biol.* 109:3259–3272.
27. Pelham, H. R. B. 1991. Multiple targets for brefeldin A. *Cell.* 67:449–451.
28. Reaves, B., and G. Banting. 1992. Pertubation of the morphology of the trans-Golgi network following Brefeldin A treatment: redistribution of a TGN-specific integral membrane protein, TGN38. *J. Cell Biol.* 116: 85–94.
29. Sandberg, P.-O., L. Marzella, and H. Glaumann. 1980. A method for rapid isolation of rough and smooth microsomes and Golgi apparatus from rat liver in the same sucrose gradient. *Exp. Cell Res.* 130:393–400.
30. Sandvig, K., and S. Olsnes. 1979. Effect of temperature on the uptake, excretion and degradation of abrin and ricin by HeLa cells. *Exp. Cell Res.* 121:15–25.
31. Sandvig, K., T. I. Tønnessen, and S. Olsnes. 1986. Ability of inhibitors of glycosylation and protein synthesis to sensitize cells to abrin, ricin, Shigella toxin, and Pseudomonas toxin. *Cancer Res.* 46:6418–6422.
32. Sandvig, K., K. Prydz, S. H. Hansen, and B. van Deurs. 1991. Ricin transport in brefeldin A treated cells: correlation between Golgi structure and toxic effect. *J. Cell Biol.* 115:971–981.
33. Sandvig, K., K. Prydz, M. Ryd, and B. van Deurs. 1991. Endocytosis and intracellular transport of the glycoplipid-binding ligand Shiga toxin in polarized MDCK cells. *J. Cell Biol.* 113:553–562.
34. Sandvig, K., K. Prydz, and B. van Deurs. 1992. Endocytic uptake of ricin and Shiga toxin. *In* Endocytosis. From Cell Biology to Health, Disease and Therapy. P. J. Courtoy, editor. Springer Verlag, New York. 405–412.
35. Steinman, R. M., S. E. Brodie, and Z. A. Cohn. 1976. Membrane flow during pinocytosis. A stereologic analysis. *J. Cell Biol.* 68:665–687.
36. Tooze, J., and M. Hollinshead. 1991. Tubular early endosomal networks in AtT20 and other cells. *J. Cell Biol.* 115:635–653.
37. van Deurs, B., L. R. Pedersen, A. Sundan, S. Olsnes, and K. Sandvig. 1985. Receptor-mediated endocytosis of a ricin-colloidal gold conjugate in vero cells. Intracellular routing to vacuolar and tubulo-vesicular portions of the endosomal system. *Exp. Cell Res.* 159:287–304.
38. van Deurs, B., T. I. Tønnessen, O. W. Petersen, K. Sandvig, and S. Olsnes. 1986. Routing of internalized ricin and ricin conjugates to the Golgi complex. *J. Cell Biol.* 102:37–47.
39. van Deurs, B., O. W. Petersen, S. Olsnes, and K. Sandvig. 1987. Delivery of internalized ricin from endosomes to cisternal Golgi elements is a discontinuous, temperature-sensitive process. *Exp. Cell Res.* 171:137–152.
40. van Deurs, B., Z.-Z. Zou, P. Briand, Y. Balslev, and O. W. Petersen. 1987. Epithelial membrane polarity: a stable, differentiated feature of an established human breast carcinoma cell line MCF-7. *J. Histochem. Cytochem.* 35:461–469.
41. van Deurs, B., O. W. Petersen, S. Olsnes, and K. Sandvig. 1989. The ways of endocytosis. *Int. Rev. Cytol.* 117:131–177.
42. van Deurs, B., S. H. Hansen, O. W. Petersen, E. L. Melby, and K. Sandvig. 1990. Endocytosis, intracellular transport and transcytosis of the toxic protein ricin by a polarized epithelium. *Eur. J. Cell Biol.* 51:96–109.
43. von Bonsdorff, C.-H., S. D. Fuller, and K. Simons. 1985. Apical and basolateral endocytosis in Madin-Darby canine kidney (MDCK) cells grown on nitrocellulose filters. *EMBO (Eur. Mol. Biol. Organ.) J.* 4:2781–2792.
44. Wood, S. A., J. E. Park, and W. J. Brown. 1991. Brefeldin A causes a microtubule-mediated fusion of the *trans*-Golgi network and early endosomes. *Cell.* 67:591–600.